MU3 (Contributed Oral)
2:00 PM – 2:15 PM

Real-time Comparison of Blind Phase Search with Different Angle Resolutions for 16-QAM

A. Al-Bermani[(1)], C. Wördehoff[(2)], O. Jan[(1)], K. Puntsri[(1)], U. Rückert[(2)], R. Noé[(1)]
(1) University of Paderborn, EIM-E, Warburger Str. 100, D-33098 Paderborn, Germany
(2) Bielefeld University, CITEC, Universitätsstr. 21, D-33615 Bielefeld, Germanyalbermani /omar / puntsri@ont.upb.de; cwoerdeh@cit-ec.uni-bielefeld.de; rueckert@techfak.uni-bielefeld.de; noe@upb.de

Abstract-- *The influence of phase noise related to 16 and 32 test carrier phase angles of BPS carrier recovery in a 16-QAM transmission system has been investigated in real-time with a data rate of 2.5 Gb/s.*

Index Terms—Optical communication, Quadrature amplitude modulation, Coherent communication, Phase estimation, Feedforward carrier recovery.

I. Introduction

The use of multi-level modulation formats, usually with coherent detection, is one of the most effective methods of increasing the bit rate in optical fiber transmission systems while the symbol rate is maintained. It has allowed reaching transmission rates of 112 Gb/s and above. Among the possible formats 16ary quadrature amplitude modulation (16-QAM) which carries 4 bit/symbol is an attractive candidate. Recently, simulations, offline and real-time experiments with this modulation format have been performed [1-4]. Based on our phase-noise tolerant QAM carrier recovery algorithm [5], we present results of a 2.5 Gb/s real-time transmission experiment with synchronous digital detection of a 16-QAM constellation. We test phase noise tolerance for blind phase search (BPS) feedforward carrier recovery with alternatively 16 and 32 test phase angles. Signals are processed digitally in real-time on a field-programmable gate array (FPGA).

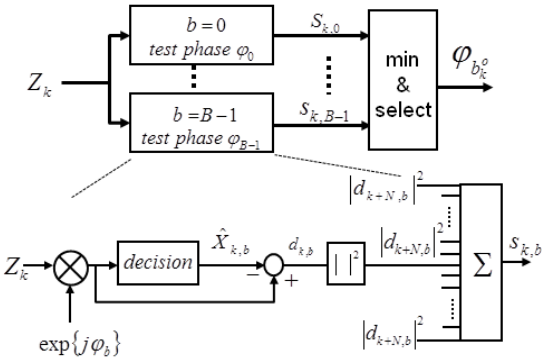

Fig. 1. BPS feedforward carrier and data recovery using B test phase values φ_b

II. Blind Phase Search Carrier Phase Estimator

Fig. 1 shows a block diagram of the realized carrier recovery module. The estimator simultaneously tries a fixed set of B carrier phase angles in a quadrant and determines the most likely one of them. The squared distance between the recovered 16-QAM symbol and the closest constellation point is filtered over $2N+1$ consecutive symbols. That test phase angle for which the filtered squared distance is minimum yields the correct constellation point within a quadrant. BPS is very robust against ASE noise but the complexity increases with the number of test angles because the decision circuit has to be implemented B times.

III. Experimental Setup

The experimental setup of our coherent transmission system is shown in Fig. 2. The transmitter consists of a data source and driver amplifiers. The transmitter comprises a commercial external cavity laser (ECL) having a line width of approximately 150 kHz and an IQ modulator driven by two 625 Mbaud quaternery data streams which are generated by an FPGA. The data is first mapped to the constellation points before the quadrant number is differentially precoded to cope with quadrant phase slips during receiver-side carrier synchronization. The generated waveforms are passively combined to form two 4-level 625-Mbaud electrical waveforms for in-phase (I) and quadrature (Q) modulation. The levels of the most and least significant bit (MSB, LSB) are coarsely set using fixed 6-dB attenuators in one path. The IQ modulator is a double-nested Mach–Zehnder modulator based on $LiNbO_3$. The electrical constellation before optical transmission is shown as an inset in Fig. 2. The constellation diagram shows clear transitions. After transmission through 20 or 81 km of standard single-mode fiber the signal is fed to a variable optical attenuator (VOA) followed by an EDFA and a ~20 GHz wide bandpass filter for noise filtering. The optical signal before (b) and after (c and d) transmission is analyzed using an oscilloscope with a photodiode. Polarization is controlled manually. On the receiver side, the signal is mixed with local oscillator (LO) laser utilizing a 90° optical hybrid. Two differential photodiode pairs convert the signal from optical to electrical (O/E). After photodetection and linear amplification the signals are converted to the digital domain. The ADC performance is one of the barriers that can limit the total data rate of a DSP-based optical coherent systems. The electrical constellation after optical transmission is shown as insets in (e and f). The ADCs utilized in this setup are commercially available with 4, 5 and 6-bit data converters at the symbol rate of 625 MHz.

The signal processing is implemented in XilinxVirtex 6 FPGA where electronic carrier and data recovery signals are processed in real-time. Interconnections between the ADCs and the FPGA are implemented in low-voltage differential signaling (LVDS). The carrier phase and frequency need to be recovered before a decision on the symbol can be made. Phase estimation was implemented as BPS with B = 16 and B = 32 test carrier phase angles. In our design N = 6 temporal samples before and after the current sample are processed to recover the carrier. The optimum phase angle is determined by searching the minimum sum of distance values. DSP in the FPGA is performed in M = 8 parallel streams after demultiplexing. All the results of the bit streams are measured in real-time. To perform bit-error-rate (BER) measurements, an appropriate bit pattern is programmed into the BER tester.

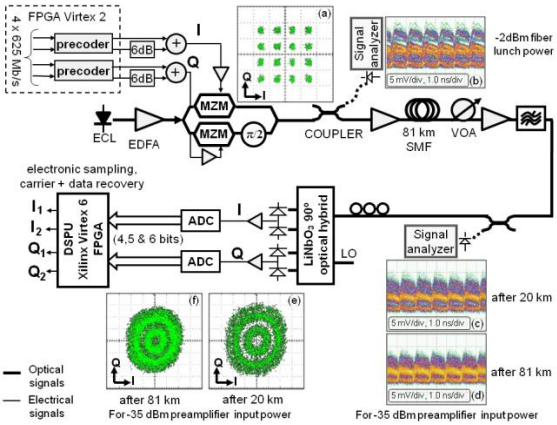

Fig. 2. 16-QAM transmission setup with real-time synchronous coherent digital I&Q receiver.

IV. Measurement Results

Fig. 3 shows BER vs. received power for 2.5 Gbit/s transmission over distances of 20 and 81 km, using 2^7-1 PRBS data. The best measured BER was $2.5 \cdot 10^{-4}$ and $3.1 \cdot 10^{-4}$ for 20 km of fiber, for B = 32 and B = 16 respectively. Both DSP setups could be detected until the preamplifier input power was set below −45 dBm. The BER floors for 81 km distance are slightly higher than for 20 km, $1.04 \cdot 10^{-3}$ and $1.5 \cdot 10^{-3}$ for B = 32 and B = 16 test phase angles, respectively. This is probably due to the lack of a clock recovery circuit in the receiver and the resulting usage of the transmitter clock, which introduced sampling phase noise. We can observe a 1 dB penalty in the BER curve between B =32 and B = 16 to the RX input power for 20 km and 2.5 dB for 81 km of fiber length. Fig. 4 shows the Q-factor dependence on fiber input power over 81 km of optical transmission for different ADC resolutions. The Q-limit for a state-of-the-art FEC (7% overhead) is plotted as a dashed line. Up to –20 dBm received preamplifier input power a 1-dB performance penalty between B =32 and B = 16 can be observed for 6-bit ADC resolutions, while the penalty is increased as we decrease the ADC resolution.

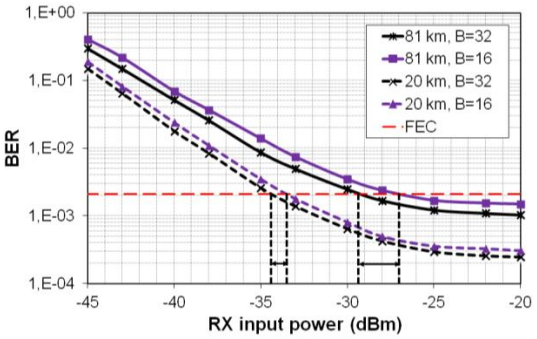

Fig. 3. Measured BER vs. optical power at the preamplifier input, averaged over all 4 subchannels (I1, Q1, I2 and Q2) at 2.5 Gbit/s data rate for 16 and 32 test phase angle numbers, $\Delta f \cdot T$ = 0.00048.

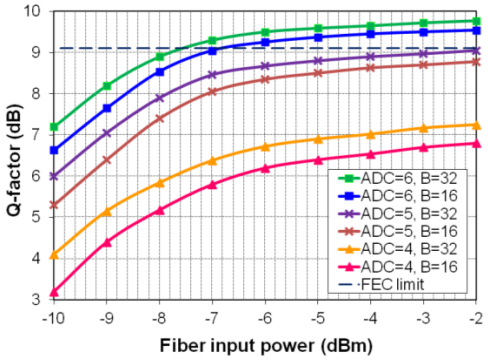

Fig. 4. Q-factor vs. fiber input power for different ADC resolutions and different test phase angle numbers. Fiber length was 81 km.

V. Summary

We have demonstrated a real-time comparison of BPS feedforward carrier phase estimation with different numbers of test phase angles. 2.5 Gbit/s 16-QAM data was transmitted over 20 and 81 km of fiber in a self-homodyne configuration with an ECL. These results underline the excellent robustness of BPS with 32 test carrier phase angles in the square 16-QAM modulation format. The averaged BER was below the threshold of a state-of-the-art FEC (7% overhead) for receiver input powers above −30 dBm.

References

[1] L. Molle et al., " Polarization Multiplexed 20 Gbaud Square 16QAM Long-Haul Transmission over 1120 km using EDFA Amplification," We 8.4.4, ECOC 2009, 20-24 September, Vienna, Austria, 2009.

[2] P. Winzer, et al., "Generation and 1,200-km Transmission of 448-Gb/s ETDM 56-Gbaud PDM 16-QAM using a Single I/Q Modulator," Europ. Conf. on Optical Comm. (ECOC), 2010, paper PD2.2.

[3] T. Pfau et al., "Towards Real-Time Implementation of Coherent Optical Communication," Proc. OFC/NFOEC 2009, March 22-26, 2009, invited paper, OThJ4, San Diego, CA, USA.

[4] A. Al-Bermani et al., "Synchronous Demodulation of Coherent 16-QAM with Feedforward Carrier Recovery," Journal of IEICE, Vol.E94-B,No.07,Jul. 2011.

[5] T. Pfau, S. Hoffmann, and R. Noe, "Hardware-efficient coherent digital receiver concept with feedforward carrier recovery for M-QAM constellations," J. Lightw. Technol., vol. 27, no. 8, pp. 989-999, Apr. 15, 2009.